

Krill availability in adjacent Adélie and gentoo penguin foraging regions near Palmer Station, Antarctica

Schuyler C. Nardelli ^{1*}, Megan A. Cimino ², John A. Conroy ³, William R. Fraser ⁴,
Deborah K. Steinberg ³, Oscar Schofield ¹

¹Department of Marine and Coastal Sciences, Rutgers University's Center for Ocean Observing Leadership (RU COOL), Rutgers, The State University of New Jersey, New Brunswick, New Jersey

²Institute of Marine Science, University of California, Santa Cruz, California

³Virginia Institute of Marine Science, William & Mary, Gloucester Point, Virginia

⁴Polar Oceans Research Group, Sheridan, Montana

Abstract

The Palmer Deep canyon along the West Antarctic Peninsula is a biological hotspot with abundant phytoplankton and krill supporting Adélie and gentoo penguin rookeries at the canyon head. Nearshore studies have focused on physical mechanisms driving primary production and penguin foraging, but less is known about finer-scale krill distribution and density. We designed two acoustic survey grids paired with conductivity–temperature–depth profiles within adjacent Adélie and gentoo penguin foraging regions near Palmer Station, Antarctica. The grids were sampled from January to March 2019 to assess variability in krill availability and associations with oceanographic properties. Krill density was similar in the two regions, but krill swarms were longer and larger in the gentoo foraging region, which was also less stratified and had lower chlorophyll concentrations. In the inshore zone near penguin colonies, depth-integrated krill density increased from summer to autumn (January–March) independent of chlorophyll concentration, suggesting a life history-driven adult krill migration rather than a resource-driven biomass increase. The daytime depth of krill biomass deepened through the summer and became decoupled from the chlorophyll maximum in March as diel vertical migration magnitude likely increased. Penguins near Palmer Station did not appear to be limited by krill availability during our study, and regional differences in krill depth match the foraging behaviors of the two penguin species. Understanding fine-scale physical forcing and ecological interactions in coastal Antarctic hotspots is critical for predicting how environmental change will impact these ecosystems.

The West Antarctic Peninsula is characterized by high summer primary productivity, large krill stocks, and abundant penguins, whales, and seals (Ross et al. 1996a). Although the entire inner continental shelf is highly productive, penguin colonies are distributed heterogeneously (Fraser and Trivelpiece 1996), which has been related to the presence of deep submarine canyons that extend from the continental shelf break to the land margin and transport warm (> 1°C), high-nutrient Upper Circumpolar Deep Water inshore (Couto et al. 2017). The interaction between the ocean currents and bathymetry in these canyons serves to concentrate and promote phytoplankton

growth (Kavanaugh et al. 2015; Carvalho et al. 2019), and to aggregate Antarctic krill (*Euphausia superba*), supporting large higher trophic level populations (Santora and Reiss 2011). Few studies have investigated local-scale krill distributions within these canyon hotspots and their direct impact on predator foraging ecology.

The West Antarctic Peninsula is undergoing significant warming and melting, leading to a latitudinal climate gradient with warm, moist subpolar conditions propagating south to replace cold, dry polar conditions (Stammerjohn et al. 2012; Cook et al. 2016). The Palmer Deep submarine canyon, located near the U.S. research base Palmer Station, is in the transition zone between polar and subpolar climates, making it an ideal location to study ecosystem changes. Polar, ice-obligate Adélie penguins (*Pygoscelis adeliae*) have high breeding site fidelity and natal philopatry (i.e., they repeatedly return to their birthplace to breed), and colonies in the Palmer region have existed for hundreds to thousands of years (Emslie 2001). With sea ice loss and increased snowfall, local

*Correspondence: nardelli@marine.rutgers.edu

This is an open access article under the terms of the Creative Commons Attribution License, which permits use, distribution and reproduction in any medium, provided the original work is properly cited.

Additional Supporting Information may be found in the online version of this article.

Adélie penguin populations have declined $\sim 90\%$ since the 1970s (Fraser et al. 2020). Concurrently, sub-Antarctic, ice-intolerant gentoo penguins (*Pygoscelis papua*) established colonies near Palmer Station in 1994 and have been increasing ever since (Fraser et al. 2020). In the Palmer region, both species feed almost exclusively on krill (Fraser and Hofmann 2003; Pickett et al. 2018), and krill abundance in the region remained relatively stable from 1993 to 2013 (Steinberg et al. 2015). However, from 1976 to 2016 there was a krill abundance decline in the southwest Atlantic sector, and a southward range contraction that concentrated krill distribution along the West Antarctic Peninsula shelf (Atkinson et al. 2019). This is notable because further warming could cause additional range contractions and decreased krill biomass near Palmer Station (Klein et al. 2018), which in turn could increase penguin foraging efforts and decrease breeding success (Fraser and Hofmann 2003; Chapman et al. 2011).

Adélie and gentoo penguins are central place foragers, and nearly a decade of penguin satellite tag data near Palmer Station shows each species forages $\sim 8\text{--}25$ km from their respective colonies within two spatially segregated foraging habitats

(Fig. 1; Cimino et al. 2016; Pickett et al. 2018). Adélie penguins breeding on Humble and Torgerson Islands forage mainly over the northern flank of the Palmer Deep canyon at shallow depths (mean 17.1 ± 8.8 m; Pickett et al. 2018). This region is characterized by fresher, coastally influenced waters with shallow mixed layer depths (MLDs), slower currents, longer residence times (1–4 d), and higher chlorophyll concentrations (Carvalho et al. 2016; Kohut et al. 2018). Gentoo penguins breeding on Biscoe Point forage over the southern flank of the canyon and into the Bismarck Strait, often at deeper depths (mean 41.5 ± 23.6 m; Pickett et al. 2018). This region is more offshore-influenced with intrusions of warm and nutrient-rich Upper Circumpolar Deep Water, deeper MLDs, faster currents, shorter residence times (0.2–2 d), and lower chlorophyll concentrations (Carvalho et al. 2016; Kohut et al. 2018). Despite the importance of krill within this ecosystem, little is known about their role linking physical and primary production dynamics to penguin foraging. Previous studies show that austral summer krill distributions in the Palmer Deep canyon are influenced by physics (e.g., tidal cycles, MLD, winds) and phytoplankton concentration

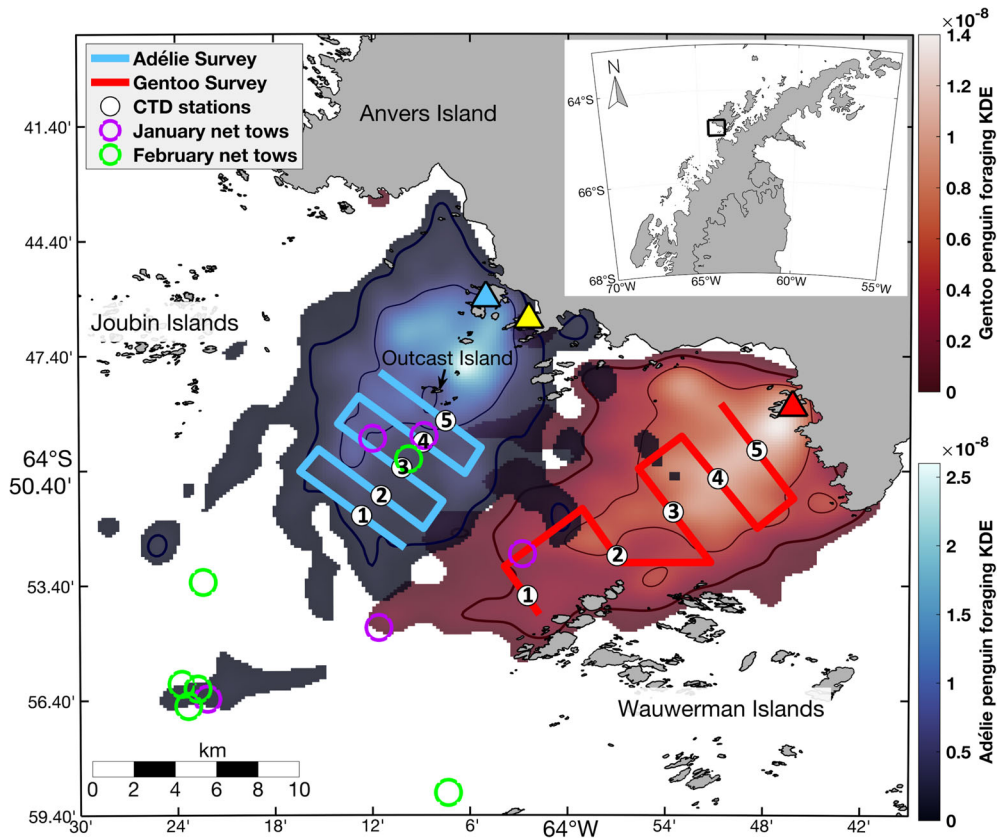


Fig 1. Map of the region south of Anvers Island along the West Antarctic Peninsula (inset) showing penguin foraging 2D kernel density estimates (KDE) based on foraging dives from satellite tag data from 2009 to 2019 (blue = Adélie foraging region, red = gentoo foraging region). The outer extent of the colored area is the 90% KDE, the thick line is the 80% KDE, and the thin line is the 50% KDE. Overlaid are the locations of the acoustic surveys, CTD profiling stations, and net tows. The blue triangle represents Adélie penguin colonies on Humble/Torgerson Islands, the red triangle represents the gentoo penguin colony on Biscoe Point, and the yellow triangle represents Palmer Station. Survey leg numbers are labeled 1–5 in black for each foraging region.

(Bernard and Steinberg 2013; Cimino et al. 2016; Bernard et al. 2017) and that foraging penguins respond to physical characteristics such as surface convergent features and tides (Oliver et al. 2013, 2019). Our study is the first to document seasonal krill dynamics specific to the two penguin foraging regions and describe differences in krill availability for the respective penguin populations. Using data collected over one austral summer, we assess (1) differences in krill availability (depth-integrated density, spatial and vertical distributions, and swarm structure) between the two penguin foraging regions; (2) associations between these patterns and regional oceanographic properties; and (3) implications for penguin foraging behavior. The surveys created for this study are the start of a new data set introduced to the Palmer Antarctica Long-Term Ecological Research (LTER) project, designed to provide data on nearshore krill distributions at spatial and temporal scales that are relevant to penguin foraging ecology. Our results emphasize the importance of organismal life histories in understanding ecological interactions over seasonal scales, which is crucial for predicting how continued environmental change will impact krill and penguin populations in ecologically important coastal areas.

Methods

Survey design

Survey design was based on 9 yr of penguin satellite tag data (2009–2018) indicating the key foraging regions for established Adélie and gentoo penguin colonies near Palmer Station. Methods for processing tag data and calculating the penguin foraging 2D kernel density estimations shown in Fig. 1 are outlined in Cimino et al. (2016) and Pickett et al. (2018). Two 20-nautical mile acoustic surveys were centered in each species' foraging region (Fig. 1). Each survey was paired with five conductivity–temperature–depth (CTD) profiling stations located midway across each northwest-southeast survey leg to collect ancillary physical oceanographic and phytoplankton data. Each survey was run weekly over one austral summer season (January–March 2019) during the daytime (approximately 9:00 to 15:00 h local) pending weather. When possible, the two surveys were run on consecutive days; however, weather sometimes increased the interval to 3 d. Two additional early-season surveys were conducted on 28 November 2018 in the Adélie region and on 18 December 2018 in the gentoo region. A total of 25 surveys were run over the season, 14 in the gentoo foraging region and 11 in the Adélie foraging region.

Acoustic data collection

Surveys were conducted aboard a 10-m-long rigid-hulled inflatable boat equipped with a hull-mounted, downward-facing Simrad EK80 single-frequency (120 kHz) transducer (Kongsberg Maritime, Kongsberg, Norway). During all surveys, 1 kW pulses at 256 ms duration were transmitted once per

second. Geographic positions were simultaneously logged using the vessel's Global Positioning System. Acoustic surveying speed averaged five knots to ensure high-quality data while allowing for the longest feasible survey distance. The system was calibrated mid-season in the field using the standard sphere method (Foote 1990), whereby a 38.1-mm tungsten-carbide calibration sphere with known acoustic properties was suspended below the transducer and moved within the acoustic beam.

Krill net sampling

To inform acoustic processing, *E. superba* were collected from the RV *Laurence M. Gould* in the Palmer Deep canyon using a 2 × 2 m square frame Metro net with 700- μ m mesh towed obliquely. Five net tows were conducted from 06 January 2019 to 08 January 2019 (three tows down to 120 m and two krill-targeted tows to 20 and 25 m, respectively), and six net tows were conducted from 03 February 2019 to 05 February 2019 (two tows to 120 m, one krill-targeted tow to 100 m, two double tow-yos to 60 m, and one double tow-yo to 75 m). Length measurements were made for a random subsample of 100 *E. superba*, or all *E. superba* caught in each tow if there were < 100 krill (standard length 1 of Mauchline 1980). Krill length–frequencies were calculated in 1-mm bins separately for January, February, and both months combined. Gaussian mixture models were fit to the three length-frequency distributions using the MATLAB function *fitgmdist*. Based on visual examination of the length-frequency histograms for the different time periods, three length modes were selected for the analysis. The model output gives the mean of each length mode and the mixing proportion for each mode (probability that an observation comes from that mode).

Acoustic data processing

Raw acoustic data from the 120-kHz transducer were processed using Myriax Echoview version 10.0. Estimated background noise levels were subtracted from the echogram, and surface noise (top 4 m) and the ocean bottom were removed before analysis. The calibration from the transducer was applied to the echogram and adjusted for speed of sound and absorption coefficients derived from CTD profiles taken during each survey.

Volume backscattering strength (dB re 1 m⁻¹) due to *E. superba* was isolated using a –70 dB threshold (Lawson et al. 2008). This threshold was estimated based on the maximum distance that krill can maintain visual contact with other krill and reflects a packing density of 1.7 ind. m⁻³. In addition to *E. superba*, the krill species *Thysanoessa macrura* was present in the study area during the survey period. In most cases, the –70 dB threshold and swarm detection parameters (see below) likely excluded *T. macrura*, which is distributed more evenly in space than *E. superba* and forms diffuse aggregations that are acoustically distinct from those of

E. superba (Daly and Macaulay 1988; Lawson et al. 2008). Therefore, the contribution of *T. macrura* to estimated krill biomass in this study is likely minor. The tunicate *Salpa thompsoni* has a similar target strength (TS) to krill (−85 to −65 dB at 120 kHz; Wiebe et al. 2010); however, during the study period, no salps were encountered in the net tows or seen floating on the surface, which is common in years when salps are abundant.

Because ~98% of krill biomass is contained in patches or swarms (Fielding et al. 2014), swarms were isolated and used for our analysis. Krill swarms were detected using the “School Detection module” in Echoview. The software detected swarms with a minimum length of 4.5 m and a height of 2 m and linked swarms within 15 m horizontally and 5 m vertically of each other. These parameters were determined based on the resolution of our acoustic data, guided by methods in Tarling et al. (2018). Detected swarms that were too small to be corrected for beam geometry were removed from the analysis (Diner 2001).

Acoustic noise limited the detection of swarms deeper than 250 m; however, this limitation should have minimal impact on our biomass estimates as most studies show that summertime krill swarms typically reside in the top 150 m of the water column (e.g., Miller and Hampton 1989). High phytoplankton productivity in summer and early fall likely resulted in little to no krill benthic feeding, which is usually a result of reduced feeding success in surface waters (Schmidt et al. 2011). Additionally, this analysis is focused on krill availability to penguins in the Palmer region, which typically forage in the top 150 m of the water column (Pickett et al. 2018).

During our 25 survey days, a total of 3521 krill swarms were detected. Individual swarm features were calculated including mean length (m), mean height (m), and area (m²). Volume backscattering strength was integrated within each krill swarm, resulting in an area backscattering coefficient (s_a ; m² m⁻²) value. Depth-integrated krill s_a values were similarly calculated by integrating volume backscattering strength from the surface to either 250 m or the seafloor, whichever was shallower, in 10-m horizontal increments along each survey track. To characterize the depth distribution of krill, volume backscattering strength was also integrated within 10-m horizontal by 1-m vertical bins for each survey, providing an s_a value for each grid cell.

The s_a values from individual krill swarms, depth-integrated survey segments, and 1-m vertical bins were all converted to density (g wet weight [WW] m⁻²) following methods in Reiss et al. (2008). Krill TS at 120 kHz was calculated using the simplified stochastic distorted-wave Born approximation model (Conti and Demer 2006) based on krill length–frequencies from either January, February, or both months combined. To remove extreme outliers, 99% of krill length–frequencies were used (Tarling et al. 2009). Surveys conducted before 17 January used January length–frequencies, surveys between 17 January

and 25 January used both months’ length–frequencies, and surveys after 25 January used February length–frequencies.

Krill density (g WW m⁻²) in individual krill swarms, depth-integrated survey segments, and 1-m vertical bins was calculated by multiplying s_a values by an area-scattering conversion factor (CF) for the respective length–frequency distribution:

$$CF = \frac{\sum_{b=1}^B f_b \times w(L_b)}{\sum_{b=1}^B f_b \times \sigma(L_b)},$$

where B is the total number of length–frequency bins, b , f_b is the frequency for each length–frequency bin, w (g per krill) is the WW of an individual krill as a function of body length (L ; mm), calculated using the model developed from Commission for the Conservation of Antarctic Marine Living Resources 2000 survey data in the Scotia Sea (Hewitt et al. 2004):

$$w = 2.236 \times 10^{-6} \times L^{3.314},$$

and σ (m² per krill) is the backscattering cross section of an individual krill as a function of body length:

$$\sigma = 10^{TS(L)/10}.$$

Total biomass (g WW) in individual krill swarms, depth-integrated survey segments, and 1-m vertical bins was calculated by multiplying the density of a krill swarm or bin by its area in m².

Environmental data

At each profiling station, CTD (SeaBird Electronics Seacat SBE 19plus sensor) and chlorophyll *a* (Chl *a*) fluorescence measurements (Wet Labs ECO fluorometer sensor) were made down to 120 m depth or within 10 m of the bottom at shallower stations. These downcast data were averaged in 1-m depth bins. Chl *a* fluorescence was calibrated against discrete water samples collected at 50 and 65 m twice per week from January to March at Palmer LTER Sta. E (located just east of Outcast Island, Fig. 1). Water samples were filtered onto Whatman GF/F filters, extracted in 90% acetone, and analyzed using a Turner fluorometer. Calibrated Chl *a* profiles were then corrected for nonphotochemical quenching using methods from Xing et al. (2012). For each profile, 50 m averaged temperature, 50 m averaged salinity, 50 m averaged particulate beam attenuation coefficient (beam *c*), 50 m integrated Chl *a*, and the depth of the chlorophyll maximum were calculated.

Since photosynthetically active radiation (PAR) measurements were not collected during surveys, 50 m averaged beam *c* measurements were compared to the depth of 1% PAR measured biweekly at Sta. E from January to March. A negative linear correlation was found between the two (Pearson’s

$r = -0.78$, $p \leq 0.001$, $n = 23$), and therefore, 50 m averaged beam c was used as a proxy for light attenuation in the surface water column.

The seasonal MLD was calculated from vertical profiles of temperature and salinity according to Carvalho et al. (2017) and is based on the depth of the maximum buoyancy frequency ($\max(N^2)$). A quality index value (QI; Lorbacher et al. 2006) was calculated for each vertical profile and was used to filter out profiles without significant stratification ($QI < 0.5$). This approach was validated using a ship-based study along the West Antarctic Peninsula (Schofield et al. 2018).

Wind speed (m s^{-1}) measurements were obtained from an automated weather station located just behind Palmer Station. 12-h averages of wind speeds were calculated for the duration of the study period using 2-min data.

Statistical analysis

All statistical analyses were conducted in MathWorks MATLAB version R2019b. Data were grouped prior to statistical analysis to address specific spatial and temporal questions. For spatial analysis, a single value for each krill variable (median swarm length, median swarm height, median swarm area, median swarm biomass, median swarm density, median krill depth, mean depth-integrated krill density, and number of krill swarms per kilometer) was calculated for each of the five survey legs in the two penguin foraging regions (see Fig. 1) for all survey days. This approach allowed pairing of the CTD and acoustic data and created equal sample sizes for all variables. For temporal analysis, a single mean or median value for each krill variable (see above) and environmental variable (mean 50 m averaged temperature, mean 50 m averaged salinity, mean 50 m integrated Chl a , mean 50 m averaged beam c , mean MLD, and mean $\max(N^2)$) was calculated for each survey day in the two penguin foraging regions. The same approach was used for the two inshore survey legs combined and the two offshore survey legs combined within each foraging region. For temporal and spatial analyses, the median krill depth was calculated using 1-m vertically binned krill densities averaged across each leg and survey. Only the 10 weeks when both surveys were conducted were included in statistical analyses to allow for a paired sample design.

Spatial differences between and within penguin foraging regions were analyzed with generalized linear mixed-effects models (GLMMs) fit by maximum likelihood (MATLAB function *fitglm*) using the single mean or median values for each survey leg. We chose GLMMs because many of the model response variables had nonnormal data distributions that generalized models can accommodate, and because mixed models can account for the temporal dependence in our data caused by our repeated, paired sample design. Each environmental and krill variable was the response variable in three different models. The first model included penguin foraging region (Adélie or gentoo) as a categorical, fixed effect to test for spatial differences between foraging regions. The other two

models included survey leg (1–5) as a continuous, fixed effect to test for inshore to offshore differences across the Adélie and gentoo regions, respectively. Sampling week was included as a random effect in all models to account for the repeated, paired sample design. For all GLMMs, appropriate model error distributions and link functions were selected by visually inspecting histograms of response variables.

Temporal trends for each penguin foraging region were analyzed with generalized linear models (GLMs; MATLAB function *fitglm*) using the single mean or median values for each survey day. Each environmental and krill variable was set as the response variable in six different models. A pair of models tested for temporal change in the full Adélie and gentoo foraging regions, respectively. A second pair of models tested for temporal change in the two inshore survey legs of the Adélie and gentoo foraging regions, respectively. A third pair of models tested for temporal change in the two offshore survey legs of the Adélie and gentoo foraging regions, respectively. All models included sampling date as a continuous, fixed variable. For all GLMs, appropriate model error distributions and link functions were selected by visually inspecting histograms of response variables.

To determine relationships between environmental and krill variables, non-parametric Kendall rank correlation tests (MATLAB function *corr*) were used due to the non-normal data distributions of most variables. Variables were paired by survey leg for correlations so that the sample size of krill variables matched the sample size of environmental variables derived from CTD profiles.

Results

Krill population characteristics

During our study, three modes of krill lengths were detected in the Palmer Deep canyon region. Juvenile krill (modes 1 and 2) accounted for 41% of total measured animals (Fig. 2A). From January to February, mode 1 shifted from 13.2 to 15.2 mm, while mode 2, centered at 21.1 mm in January, mostly disappeared from the region by early February (Fig. 2B,C). Adult krill (mode 3) accounted for 59% of total measured animals and shifted from 35.3 to 44.0 mm from January to February (Fig. 2A–C).

Spatial variability

Significant differences between the adjacent penguin foraging regions were found from January to March. The Adélie region was significantly fresher with higher $\max(N^2)$ magnitudes, higher integrated Chl a concentrations, and shallower MLDs than the gentoo foraging region (GLMM, $p \leq 0.03$; Table 1; Fig. 3A–D). The Adélie region was also marginally warmer with higher beam c values (i.e., increased light attenuation) than the gentoo foraging region (GLMM, $p = 0.13$ and 0.08 , respectively; Table 1; Fig. 3E,F). Temperatures $< 0.5^\circ\text{C}$, salinities < 33.6 , and $\max(N^2)$ values $> 1.0 \times 10^{-3}$ were all present in the Adélie region but absent in the gentoo region,

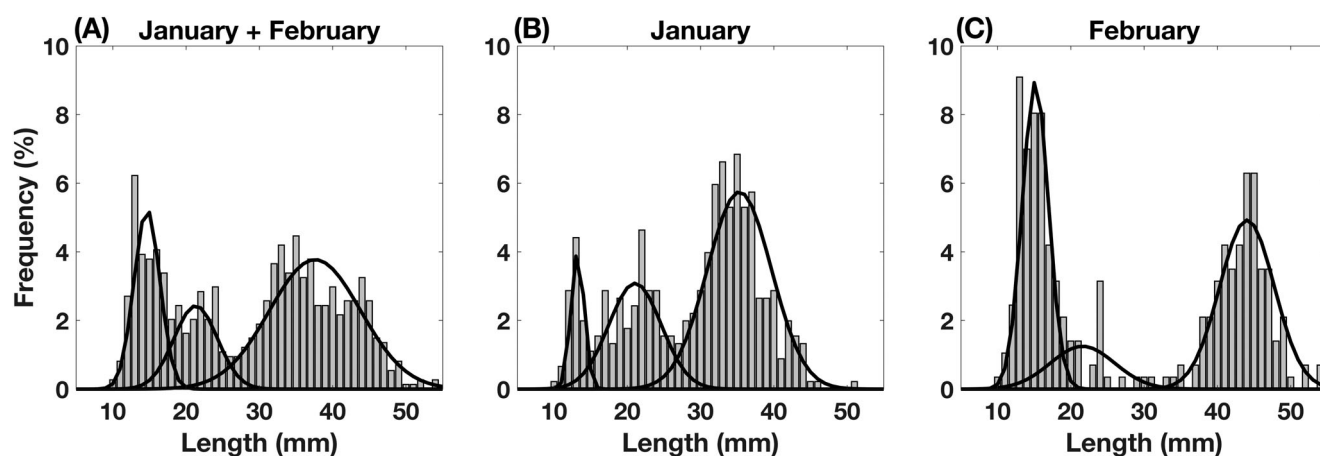


Fig 2. *Euphausia superba* length-frequency distributions in the nearshore Palmer Deep canyon for (A) January and February combined (11 net tows, 739 krill measured), (B) 06 January 2019–08 January 2019 (five net tows, 453 krill measured), and for (C) 03 February 2019–05 February 2019 (six net tows, 286 krill measured). Black lines indicate the best component fits for each krill mode based on Gaussian mixture models.

Table 1. Results from GLMMs assessing the differences in variables between Adélie and gentoo penguin foraging regions. Models for 50 m averaged temperature and 50 m averaged salinity used a normal distribution and identity link function while all other models used a gamma distribution and log link function. Significant results are indicated in bold. Weather occasionally prevented profiling at some CTD stations, and some MLD profiles failed to meet the QI threshold, resulting in $n < 50$ for those CTD-derived variables.

Variable	Adélie (n)	Gentoo (n)	Coeff.	SE	t	p
50 m averaged temperature ($^{\circ}\text{C}$)	45	49	-0.08	0.05	-1.51	0.13
50 m averaged salinity (PSU)	45	49	0.10	0.02	6.78	< 0.001
50 m integrated chlorophyll a (mg m^{-2})	45	49	-0.18	0.08	-2.19	0.03
50 m averaged beam c (m^{-1})	45	49	-0.08	0.05	-1.78	0.08
MLD (m)	28	24	0.34	0.15	2.29	0.03
Max(N^2)	28	24	-0.43	0.12	-3.65	< 0.001
Krill swarm length (m)	50	50	0.39	0.09	4.53	< 0.001
Krill swarm height (m)	50	50	0.38	0.12	3.21	0.002
Krill swarm area (m^2)	50	50	0.85	0.17	4.85	< 0.001
Krill swarm biomass (g WW)	50	50	4.12	0.43	9.57	< 0.001
Krill swarm density (g WW m^{-2})	50	50	1.35	0.34	3.97	< 0.001
Median krill depth (m)	50	50	0.11	0.14	0.84	0.41
Depth-integrated krill density (g WW m^{-2})	50	50	0.28	0.28	0.98	0.33
Number of krill swarms per kilometer	50	50	-0.16	0.14	-1.12	0.27

indicating a greater influence of surface meltwater in the Adélie region (Fig. 3A,B,E).

Krill swarms in the gentoo foraging region were longer, thicker, larger, denser, and contained higher biomass than swarms in the Adélie region (GLMM, $p \leq 0.002$; Table 1; Fig. 4A–E). Additionally, fewer krill swarms were encountered when the Chl a concentration was low (Kendall, $p = 0.01$, $\tau = 0.18$, $n = 94$), and these swarms were longer and larger (Kendall, $p \leq 0.001$ and 0.002 , $\tau = -0.28$, and -0.21 , $n = 94$ and 94 , respectively). Despite differences in krill swarm structure, there were no significant differences in the median krill depth, depth-integrated krill density, or the number of krill swarms per kilometer between foraging regions (GLMM,

$p \geq 0.27$; Table 1; Fig. 4F–H). Although the difference in median krill depth was not statistically significant, the median value in the Adélie region was 28 m shallower than in the gentoo region (55 vs. 83 m; Fig. 4F), which is similar to the 24.4 m difference in mean penguin foraging dive depths between the two regions (17.1 m for Adélie penguins and 41.5 m for gentoo penguins; Pickett et al. 2018).

There was less variability within each foraging region than between them. There were no significant differences across survey legs for environmental variables in either region (GLMM, $p \geq 0.15$; Supporting Information Table S1) or for krill variables in the gentoo foraging region (GLMM, $p \geq 0.14$; Table 2). However, in the Adélie region, depth-integrated krill

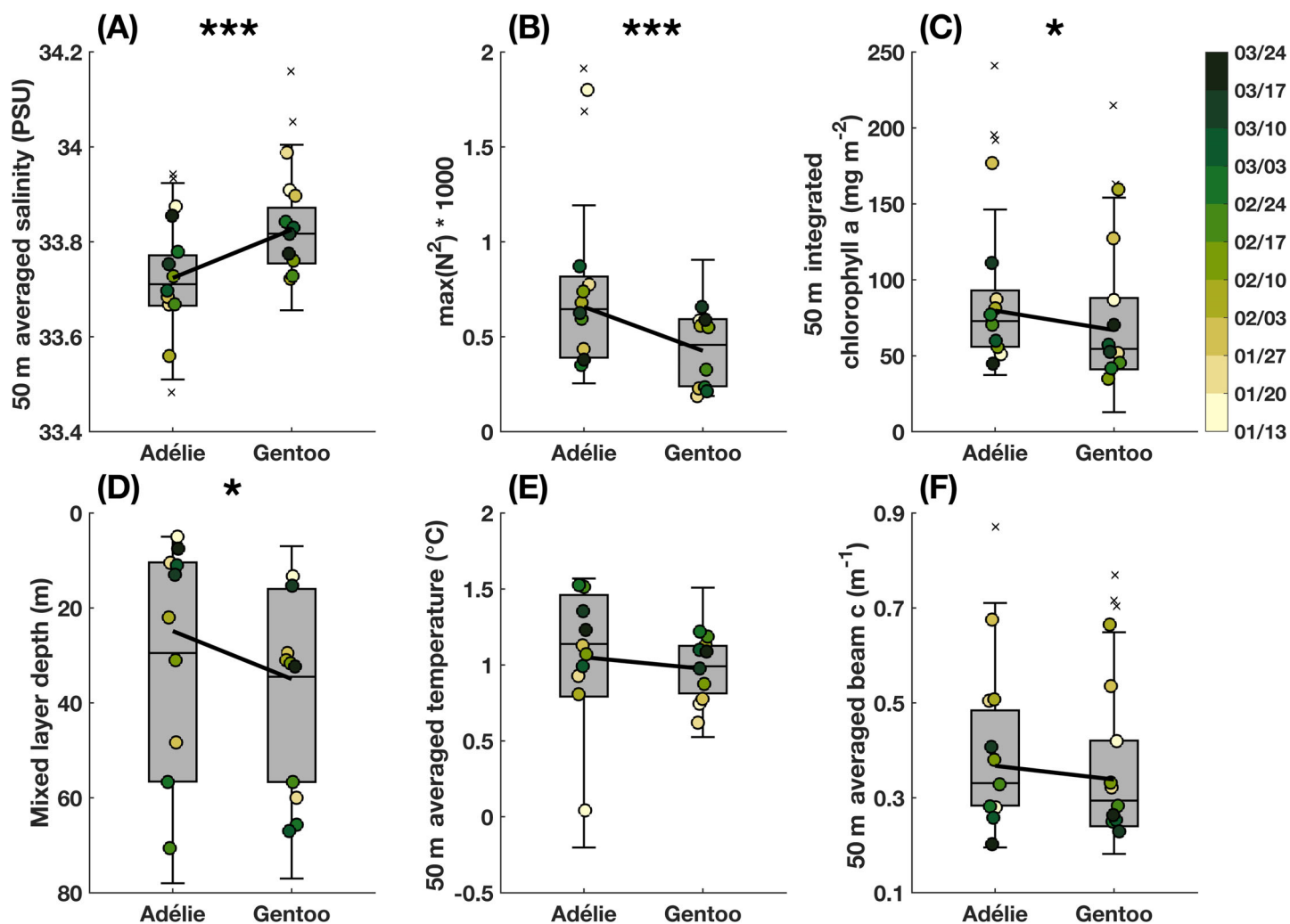


Fig 3. Differences in (A) 50 m averaged salinity, (B) $\max(N^2)$, (C) 50 m integrated chlorophyll *a*, (D) MLD, (E) 50 m averaged temperature, and (F) 50 m averaged beam *c* between the Adélie and gento survey regions. In each box plot, the horizontal line represents the median value, the top and bottom box limits represent the 25th and 75th percentiles, whiskers represent the full range of non-outlier observations, and multiplication (×) symbols represent outliers. The colored points are the mean values for each paired sampling day. Black lines indicate GLMM fits and asterisks indicate GLMM significance levels in Table 1 (* $0.01 < p \leq 0.05$, *** $p \leq 0.001$, absence of asterisks indicates $p > 0.05$). See Table 1 for *n* values.

density was highest inshore where there were more krill swarms per kilometer (GLMM, $p \leq 0.003$; Table 2; Fig. 5A,B). This heightened inshore density existed despite individual swarms being less dense and containing less biomass on the inshore survey legs (GLMM, $p \leq 0.004$; Table 2; Fig. 5C,D). Krill distribution was also deepest inshore in the Adélie region (GLMM, $p = 0.01$; Table 2; Fig. 5E).

Spatiotemporal variability in krill density

The temporal trends of environmental and krill variables inshore vs. offshore were mostly similar. For example, median krill depth deepens over time both inshore and offshore in both regions (GLM, $p \leq 0.005$; Supporting Information Tables S2 and S3). However, the temporal trends in depth-integrated krill density showed different patterns inshore

vs. offshore. In the first half of our paired sampling period (13 January–16 February), depth-integrated krill density was highest in the gento region, and biomass was concentrated in the offshore survey legs near the Wauwerman Islands (Fig. 6A). In the second half of our study period (17 February–23 March), krill density was highest at the inshore survey legs in both regions (Fig. 6B). Although krill density was variable week to week, increasing trends in krill density for the inshore survey legs and decreasing trends for the offshore survey legs in both foraging regions suggest an inshore redistribution of krill biomass from January to March (Fig. 6C,D).

Seasonal patterns

Despite significant environmental differences between the two foraging regions, seasonal patterns were similar (Fig. 7A,B,

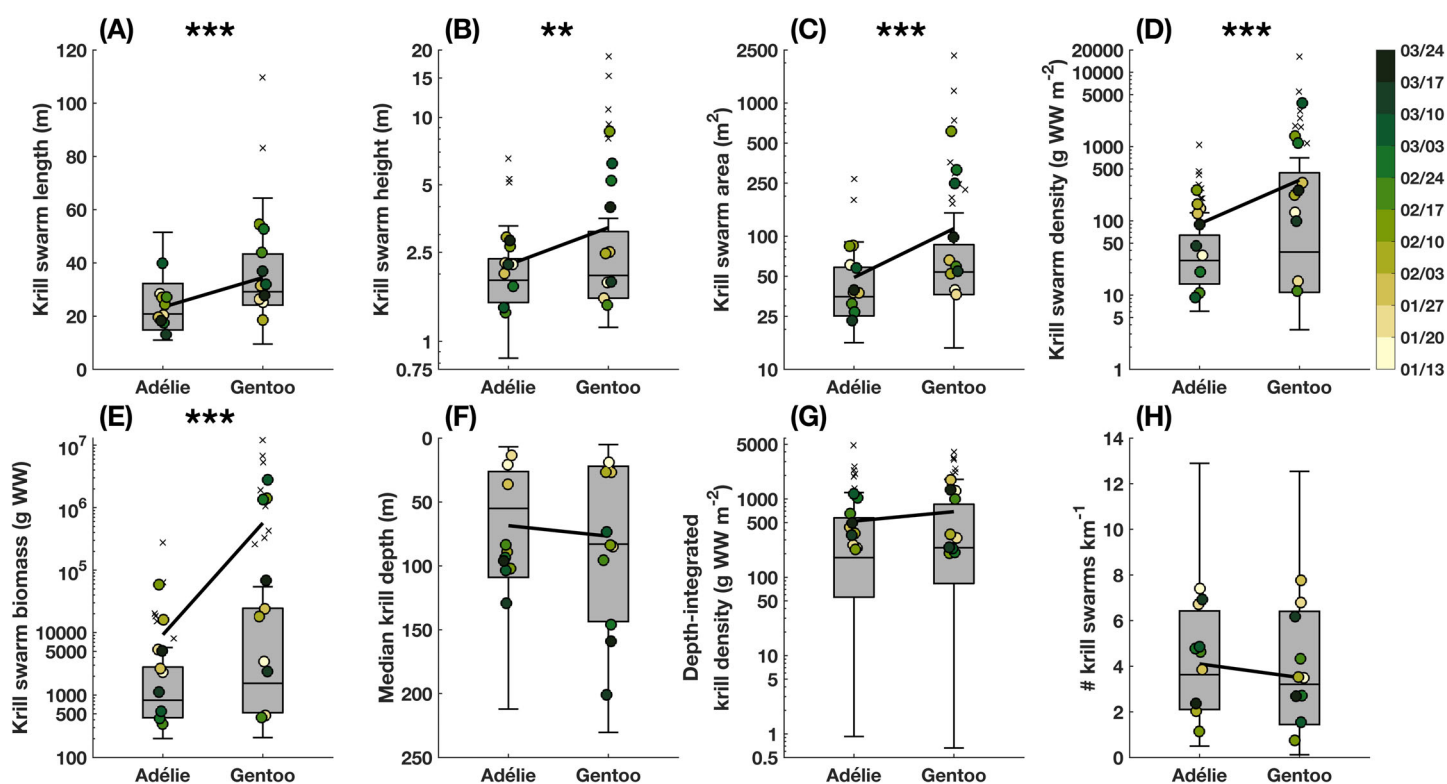


Fig 4. Differences in (A) krill swarm length, (B) krill swarm height, (C) krill swarm area, (D) krill swarm density, (E) krill swarm biomass, (F) median krill depth, (G) depth-integrated krill density, and (H) the number of krill swarms per kilometer between the Adélie and gentoo survey regions. In each box plot, the horizontal line represents the median value, the top and bottom box limits represent the 25th and 75th percentiles, whiskers represent the full range of nonoutlier observations, and multiplication (x) symbols represent outliers. The colored points are the mean values for each paired sampling day. Black lines indicate GLMM fits and asterisks indicate GLMM significance levels in Table 1 (** $p \leq 0.01$, *** $p \leq 0.001$, absence of asterisks indicates $p > 0.05$). See Table 1 for n values.

Table 2. Results from GLMMs assessing the differences in krill variables across survey legs within each penguin foraging region (Adélie and gentoo). All models used a gamma distribution and log link function. Significant results are indicated in bold. $n = 10$ for all legs in each region.

Variable	Adélie region				Gentoo region			
	Coeff.	SE	t	p	Coeff.	SE	t	p
Krill swarm length (m)	0.04	0.03	1.38	0.18	0.008	0.04	0.17	0.86
Krill swarm height (m)	-0.05	0.04	-1.49	0.14	-0.10	0.06	-1.47	0.15
Krill swarm area (m ²)	-0.06	0.05	-1.08	0.29	-0.15	0.10	-1.51	0.14
Krill swarm biomass (g WW)	-0.48	0.14	-3.49	0.001	-0.23	0.27	-0.83	0.41
Krill swarm density (g WW m ⁻²)	-0.28	0.09	-3.06	0.004	-0.20	0.20	-1.01	0.32
Median krill depth (m)	0.15	0.06	2.61	0.01	-0.07	0.05	-1.44	0.16
Depth-integrated krill density (g WW m ⁻²)	0.37	0.12	3.12	0.003	-0.02	0.15	-0.13	0.90
Number of krill swarms per kilometer	0.14	0.04	3.45	0.001	0.10	0.08	1.31	0.20

D,E). Surface freshwater pulses throughout the season stabilized the water column (increased $\max(N^2)$; Kendall, $p = 0.01$, $\tau = -0.24$, $n = 52$) and spurred phytoplankton blooms (Kendall, $p = 0.008$, $\tau = -0.19$, $n = 94$). In January, relatively calm winds (mean 2.8 m s^{-1}) and the presence of surface meltwater (0–10 m) resulted in shallow MLDs (mean Adélie = 7.8 m;

mean gentoo = 12.3 m) and high $\max(N^2)$ values (mean Adélie = 0.001; mean gentoo = 6.9×10^{-4}). On 24 January, a peak in wind speed (12.8 m s^{-1}) deepened respective MLDs to 48.3 and 60.0 m in the Adélie and gentoo regions, concurrent with increases in integrated Chl a from respective averages of 69.1 and 61.7 mg m^{-2} before the wind event to peaks of 176.8 and

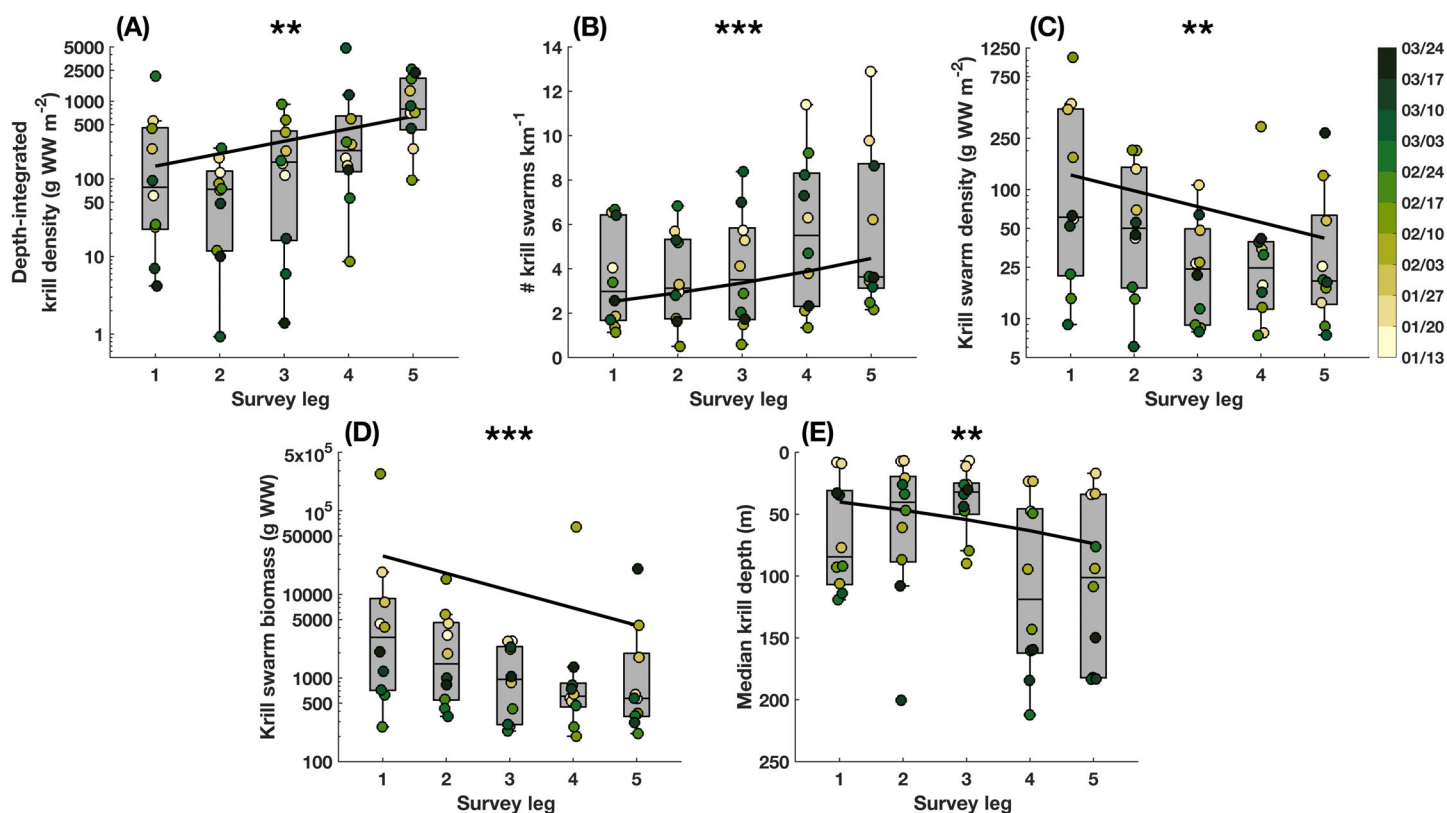


Fig 5. Differences in (A) depth-integrated krill density, (B) the number of krill swarms per kilometer, (C) krill swarm density, (D) krill swarm biomass, and (E) median krill depth across the five survey legs of the Adélie survey, with survey leg 1 located offshore and leg 5 located inshore. In each box plot, the horizontal line represents the median value, the top and bottom box limits represent the 25th and 75th percentiles, and whiskers represent the full range of non-outlier observations. The colored points are the values for each paired sampling day. Black lines indicate GLMM fits and asterisks indicate GLMM significance levels in Table 2 (** $p \leq 0.01$, *** $p \leq 0.001$, absence of asterisks indicates $p > 0.05$). $n = 10$ for all.

159.5 mg m⁻² just after the wind event. MLDs deepened to 70.6 and 67.0 m in the Adélie and gentoo regions, respectively, in late February due to higher wind speeds in the first half of February (mean 4.8 m s⁻¹). In response, phytoplankton biomass decreased to an average of 70.4 and 41.7 mg m⁻². Calmer winds in late February and early March (mean 2.5 m s⁻¹) and a small surface meltwater layer reduced MLDs in mid-March (Adélie = 10.5 m; gentoo = 28.6 m), leading to a secondary small bloom (Adélie = 111.1 mg m⁻²; gentoo = 111.9 mg m⁻²).

Krill biomass deepened significantly in both regions (GLM, $p \leq 0.005$; Supporting Information Table S4; Fig. 7C,F), especially following the primary phytoplankton bloom. The median krill depth increased from an average of 21.4 and 47.6 m in January to an average of 165.7 and 149.5 m in March for the Adélie and gentoo regions, respectively. Deeper median krill depths were correlated with lower integrated Chl *a* concentrations (Kendall $p \leq 0.001$, $\tau = -0.26$, $n = 94$) and lower beam *c* values (Kendall $p \leq 0.001$, $\tau = -0.37$, $n = 94$). In both regions, the median krill depth remained closer to the depth of the chlorophyll maximum through the primary bloom (Adélie = 8.4 m and gentoo = 28.5 m average depth

differences) than post-bloom when the difference between the two became larger (Adélie = 84.4 m and gentoo = 73.5 m differences in February; Adélie = 152.6 m and gentoo = 137.7 m differences in March), indicating a decoupling of krill biomass from the chlorophyll maximum (Fig. 7B,C,E,F).

The date of peak penguin chick fledging (13 February for Adélie penguins and 01 March for gentoo penguins) coincides with the deepening of krill biomass in both regions (Fig. 7C, F). Percent krill biomass available within each species' observed foraging depths (0–82 m for Adélie penguins and 0–144 m for gentoo penguins) decreased from an average of 75.7 to 16.3% in the Adélie region and from 96.3 to 44.8% in the gentoo region from before to after peak fledging.

Discussion

The Adélie and gentoo penguin foraging regions are adjacent to each other in the Palmer area, with the colonies located roughly 10 km apart, yet the foraging regions have significantly different oceanographic properties and krill availability. These small-scale differences are significant to central place foraging penguins that have limited foraging ranges and

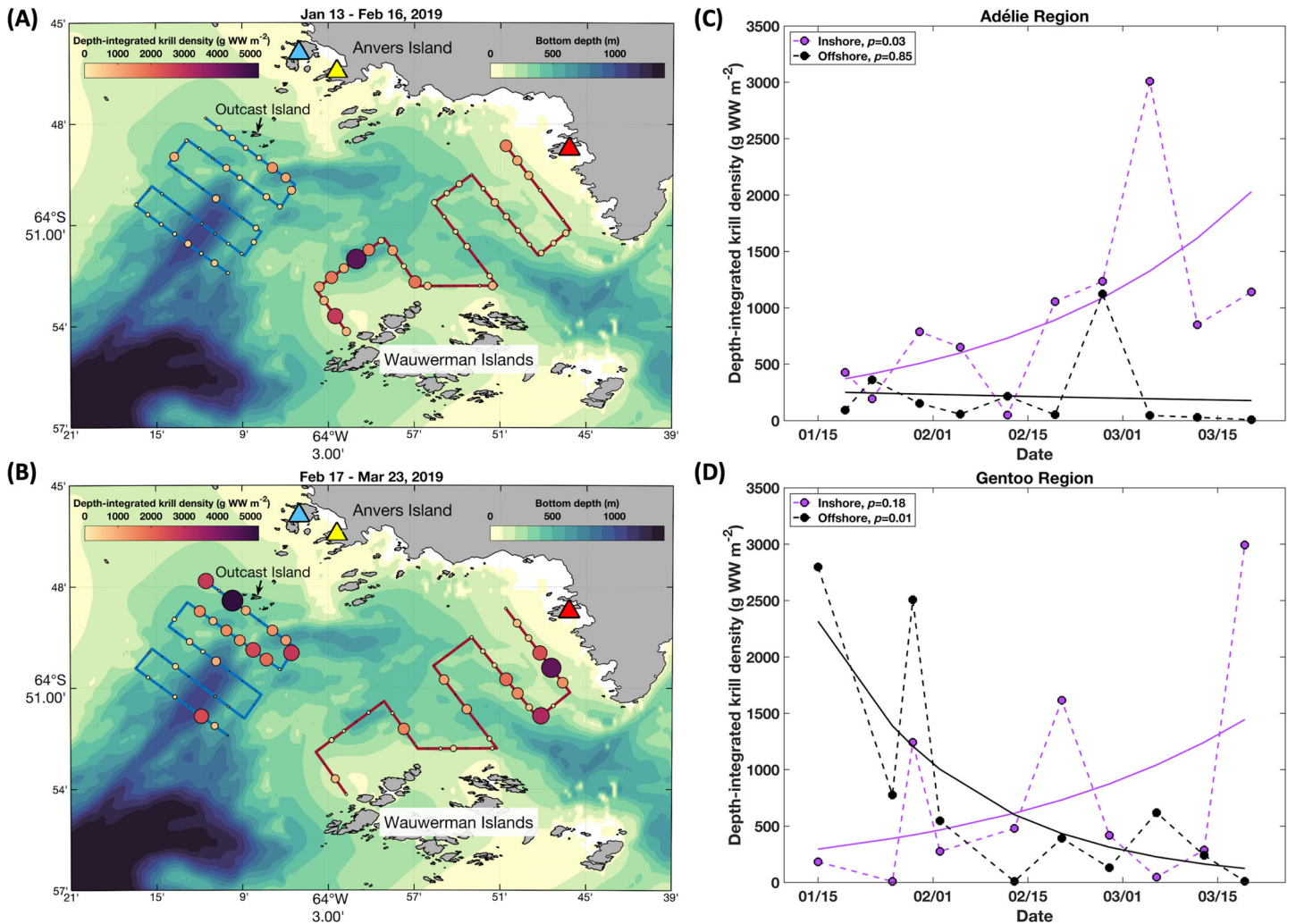


Fig 6. Seasonal spatiotemporal trends in krill biomass. Maps of mean depth-integrated krill density with the size of the circle scaled to density for roughly 1-month periods during the early and late austral summer: **(A)** 13 January 2019–16 February 2019 ($n = 5$ surveys) and **(B)** 17 February 2019–23 March 2019 ($n = 5$ surveys). The blue triangle represents Adélie penguin colonies on Humble/Torgerson Islands, the red triangle represents the gentoo penguin colony on Biscoe Point, and the yellow triangle represents Palmer Station. Time series of mean depth-integrated krill density for the inshore two survey legs (purple dots) compared to the offshore two survey legs (black dots) for the **(C)** Adélie and **(D)** gentoo penguin foraging regions. Solid lines indicate GLM fits (see Supporting Information Tables S2 and S3) with model p -values indicated in subplot legends.

are responsible for the survival of their chicks at the nest. These fine-scale and dynamic features are important in understanding differences in the foraging ecology between the local penguin populations as this polar ecosystem continues to change.

Krill population characteristics

Juvenile krill accounted for 41% of total measured animals, indicating a moderately successful recruitment year (Fig. 2; Ross et al. 2014). The prevalence of small (10–20 mm) krill during our study is unusual. Larval *E. superba* spawned the same summer would most likely be in the calyptopis stages (< 5 mm) during January/February, with relatively few having reached furcilia stages (roughly 5–15 mm; Gibbons

et al. 1999). Thus, the 10–20 mm mode is either very large age-class 0 krill or small age-class 1 krill. The latter is more likely, and two separate length modes for age-class 1 krill are sometimes reported during summer along the West Antarctic Peninsula (Ross et al. 2014).

Spatial variability

The Adélie region was fresher, had greater integrated Chl *a* and max(N^2) values, a shallower MLD, and a greater influence of coastal meltwater (Fig. 3; Table 1). The Adélie region receives greater inputs of coastal meltwater and has slower currents, resulting in a stable water column conducive to phytoplankton growth (Carvalho et al. 2016; Kohut et al. 2018). Conversely, the gentoo region receives offshore intrusions of

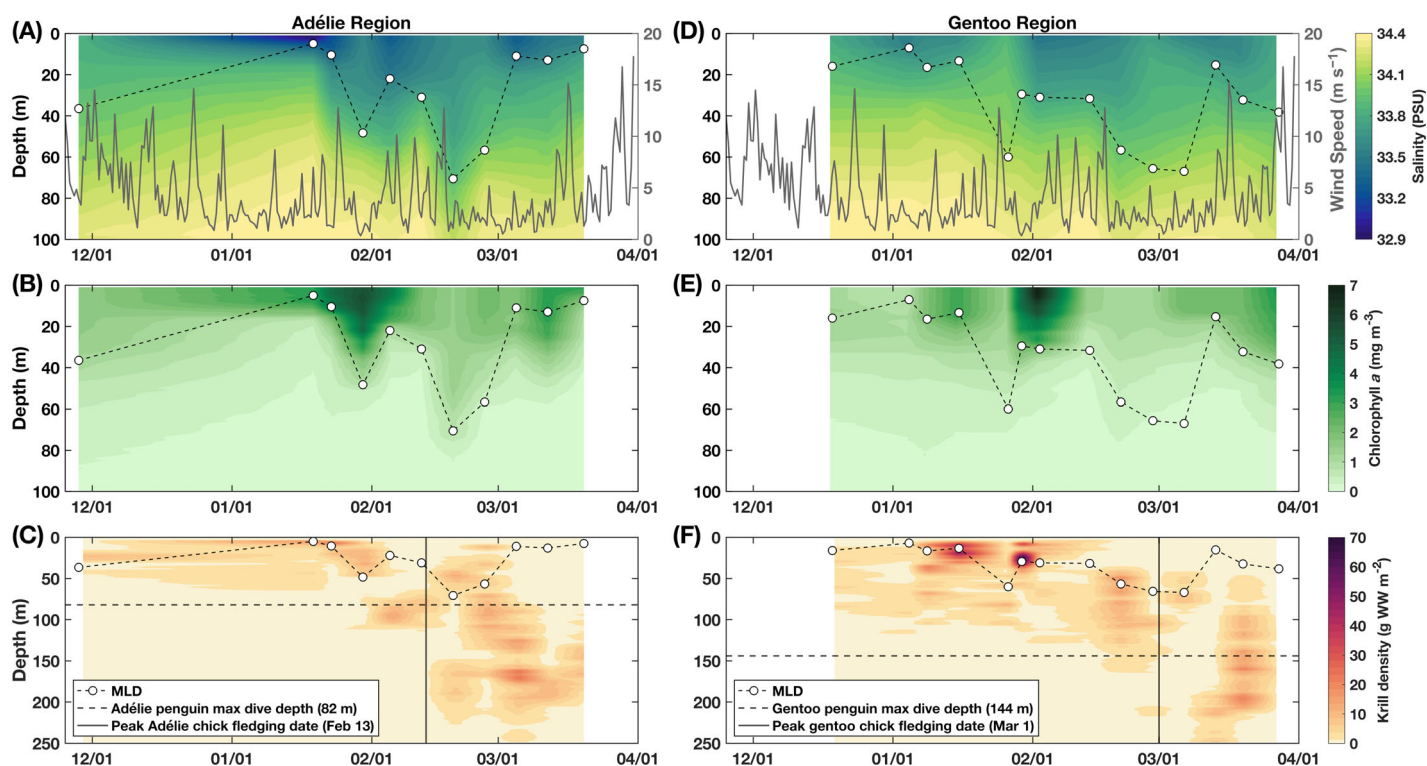


Fig 7. Time series of physical and biological properties in the (A–C) Adélie and (D–F) gentoo penguin foraging regions from November 2018 to March 2019. (A,D) Interpolated vertical cross-sections of daily averaged salinity overlaid with MLD (dashed line) and 12-h averaged wind speed (gray line). (B,E) Interpolated vertical cross-sections of daily averaged chlorophyll *a* overlaid with MLD (dashed line). (C,F) Interpolated vertical cross-sections of daily averaged krill density overlaid with MLD (dashed line). Horizontal dashed lines indicate the maximum dive depth for Adélie and gentoo penguins (82 and 144 m, respectively) based on five summers of data from Pickett et al. (2018). Vertical solid lines indicate peak penguin chick fledging dates (day when the most chicks fledged) in 2019 for each species (13 February for Adélie penguins and 01 March for gentoo penguins; methods in Chapman et al. 2010).

Upper Circumpolar Deep Water and has faster currents, which flush coastal meltwater and phytoplankton out of the region more quickly (Carvalho et al. 2016; Kohut et al. 2018).

There were no significant differences between depth-integrated krill density, the median krill depth, or the number of krill swarms per kilometer encountered in the two foraging regions; however, there were significant differences in krill swarming behavior (Fig. 4; Table 1). These patterns are significant for foraging penguins that depend on food sources proximate to their colonies. Krill swarming behavior responds to the environmental conditions that krill are experiencing, mainly to aid in finding food (Folt and Burns 1999). In the gentoo region, lower integrated Chl *a* concentrations correlated with longer and larger swarms. Previous studies in the Palmer region found krill swarms associated with low chlorophyll environments and attributed this pattern to grazing (Bernard et al. 2017) and to avoidance of high phytoplankton biomass areas that could be associated with higher predation risks (Cimino et al. 2016). Alternatively, assuming some level of organization between individuals within a swarm, a larger swarm area may increase the probability of encountering

patches of food and increase foraging efficiency, and could be a strategy to locate food in low chlorophyll environments (Hamner and Hamner 2000; Tarling et al. 2009). Greater krill densities are also found in shallower water depths and along steep bathymetric slopes (Santora and Reiss 2011; Silk et al. 2016), thus, the shallow and complex bathymetry (pinacles and seamounts) around the Wauwerman Islands may contribute to the higher-density swarms in the gentoo region.

Although not statistically significant, the median krill depth was 28 m deeper in the gentoo region than the Adélie region and was negatively correlated with Chl *a* and beam *c*. Higher integrated Chl *a* concentrations in the Adélie region increase light attenuation (reflected in higher beam *c* values) and may offer more protection from visual predators than in the gentoo region, allowing krill swarms to remain shallower. Additionally, krill may remain deeper in the gentoo region to avoid getting flushed from the region by strong surface currents (Kohut et al. 2018). Differences in krill depth distributions appear to drive differences in Adélie and gentoo foraging depths, with gentoo penguins at Biscoe Point foraging on average at deeper depths than Adélie penguins at Humble and

Torgerson Islands (41.5 and 17.1 m, respectively; Pickett et al. 2018), roughly matching the 28 m difference in median krill depth between the regions.

No significant environmental or krill differences were found across the five survey legs in the gentoo region, but in the Adélie region, there was higher depth-integrated density, more krill swarms per kilometer, and deeper krill biomass inshore compared to offshore (Fig. 5). Additionally, krill swarms inshore were less dense and contained less biomass despite the higher depth-integrated density inshore. Higher depth-integrated krill density inshore could be related to the shoaling bottom depths near Outcast Island, and deeper inshore krill biomass could be a response to increased predation closer to the Adélie penguin colonies (Klevjer et al. 2010). However, numerous low-biomass and low-density swarms inshore contradict the expectation of larger and denser swarms in the presence of visual predators (Fielding et al. 2012), such as the Adélie penguins making foraging trips from Humble and Torgerson Islands.

Spatiotemporal variability in krill density

Krill biomass dynamics operate on large spatial and temporal scales linked to their life history, with interannual variability driven by recruitment success (Reiss et al. 2008; Saba et al. 2014) and seasonal variability driven by horizontal migration (Siegel 1988; Nicol 2006). In summer, the adult krill population is concentrated near the shelf break, and juvenile krill are most abundant in coastal waters (Siegel et al. 2013; Conroy et al. 2020). In early autumn, adult krill begin moving inshore to troughs or canyons where they can utilize deep food resources during the winter (Cleary et al. 2016; Reiss et al. 2017), while juvenile and larval krill may remain shallow to access under-ice algae (Bernard et al. 2018; Walsh et al. 2020). Over our study period, krill density increased inshore in the Adélie and gentoo regions (Fig. 6) independent of changes in environmental parameters. Although there is variability in weekly krill distribution due to behavioral responses to ocean physics, food availability, and predation, the increased density inshore (especially in the Adélie region) could be linked to the inshore migration of adult krill in late summer. No net tows were available later than early February to confirm this hypothesis, but presumably we would have found a higher proportion of adult krill in those tows. The inshore increase in the gentoo region is more variable, which might reflect greater surface current speeds that may flush krill out of the region via the Bismarck Strait (Kohut et al. 2018), or the tendency of krill to aggregate near the seamounts and walls that are present along the offshore survey legs near the Wauwerman Islands.

The prevalence of juvenile krill during our study likely benefitted both penguin species. Juvenile krill remain close to shore in summer (Siegel et al. 2013; Conroy et al. 2020), causing mean depth-integrated krill density in our study to stay high throughout the summer (minimums of 111.9 and 72.7 g

WW m^{-2} for the Adélie and gentoo regions, respectively), which could lead to shorter foraging trips, chicks fed at more frequent intervals, increased chick fledging masses, and increased survival rates (Fraser and Hofmann 2003; Cimino et al. 2014). During failed recruitment years, the lack of juvenile krill inshore during summer may increase the importance of the cross-shelf adult krill migration for coastal penguin colonies and may lead to greater seasonal variability in krill biomass.

Using 12 yr of Palmer LTER data (1995–2006), Sailley et al. (2013) found that penguin colonies at Palmer Station did not appear to be limited by local krill biomass. This agrees with the results of our study. In austral summer 2018–2019, there were 1586 Adélie penguin breeding pairs (3172 potentially foraging adults) and 3655 gentoo penguin breeding pairs (7310 potentially foraging adults; W. R. Fraser unpublished). Along the West Antarctic Peninsula, past studies show average krill consumption values per foraging trip of 348.6 ($n = 48$; Volkman et al. 1980) and 510.7 g ($n = 12$; Trivelpiece et al. 1987) for Adélie penguins and 365.0 ($n = 46$; Volkman et al. 1980), 433.4 ($n = 14$; Trivelpiece et al. 1987), 671.1 (Admiralty Bay, $n = 120$; Miller et al. 2010), and 422.0 g (Cape Shirreff, $n = 130$; Miller et al. 2010) for gentoo penguins. Using the maximum average consumption estimates for each species and assuming one foraging trip a day per penguin, 3172 Adélie penguins and 7310 gentoo penguins would consume 1.6 and 4.9 tons of krill per day, respectively. Total krill biomass encountered on a given survey day (only considering our 20 nautical mile survey line) ranged from 27.2 to 1075.4 tons WW in the Adélie region and from 18.9 to 1266.6 tons WW in the gentoo region, indicating no shortage of krill for penguins within each foraging region, and plenty of prey left over for other krill predators foraging in the region such as whales, seals, fishes, and flying seabirds. In addition, Palmer region penguins forage relatively close to colonies (~ 8 – 25 km) compared to penguins in other locations where foraging trips can reach 100 km (Williams 1995), and both species are capable of much deeper dives than are seen in the Palmer region (Bost et al. 1994; Watanuki et al. 1997), further supporting that penguins do not appear to be limited by krill in this area.

Seasonal patterns

The seasonal dynamics of phytoplankton in both foraging regions match those observed over six austral summer seasons (2010–2015), with phytoplankton blooms coupled to surface meltwater dynamics (Fig. 7A,B,D,E; Carvalho et al. 2016). In late austral spring, day length is increasing, and solar warming and sea ice melt stratify the upper water column allowing phytoplankton to remain in surface waters with ample access to sunlight (Vernet et al. 2008). These conditions spur a large phytoplankton bloom in January (Carvalho et al. 2016). Following the primary bloom, decreases in meltwater inputs combined with increased wind mixing cause MLDs to deepen,

mixing phytoplankton deeper in the water column out of the range of sunlight needed for growth (Mitchell and Holm-Hansen 1991) and leading to a decline in chlorophyll concentrations. A secondary bloom in late February/early March is associated with increased freshwater input and increased water column stability, likely initiated by continued seasonal warming and glacial meltwater runoff into coastal waters (Moline and Prézelin 1996; Carvalho et al. 2016).

Similar to other Antarctic studies (Taki et al. 2005; Fielding et al. 2012), daytime krill biomass shifted deeper in the water column from January to March (Fig. 7C,F). This pattern suggests an increase in the magnitude of diel vertical migration (DVM), a behavior cued by light that balances feeding with the avoidance of visual predators (Hays 2003). During the midsummer period of near continual daylight, *E. superba* remains in surface waters to feed throughout the diel cycle and exhibits shallow or inconsistent DVM (Tarling et al. 2018). The first half of our study period is characterized by long day length (21:17–16:05 h), with high integrated Chl *a* concentrations that increase light attenuation in surface waters (as evidenced by larger beam *c* values). Although day length is long, darker daytime surface waters may offer some protection from visual predators, allowing krill to remain shallow near the depth of the chlorophyll maximum. The proximity of the median krill depth to the chlorophyll maximum in both regions through the primary bloom in late January/early February suggests krill are feeding during the daytime.

Krill DVM is typically more pronounced during spring and autumn when photoperiod is shorter (Ross et al. 1996b; Taki et al. 2005). During the second half of our study, day length was shorter (15:58–11:03 h) and integrated Chl *a* concentrations decreased, which reduced light attenuation in surface waters (as evidenced by decreased beam *c* values). Brighter daytime surface waters may make krill more susceptible to visual predators, and reduced day length increases the opportunity for protected nighttime feeding. The increased distance between median krill depth and the depth of the chlorophyll maximum in both regions after the primary bloom suggests the prioritization of daytime predator avoidance over feeding.

Adélie penguin breeding phenology is typically 2–3 weeks earlier than that of gentoo penguins, with peak fledging occurring in mid-February for Adélie penguins and in early March for gentoo penguins (Pickett et al. 2018). Obtaining high krill yields during periods of peak chick growth is critical for chick survival, and interestingly, the date of peak fledging for each species coincided with the deepening of krill biomass in their respective foraging regions (Fig. 7C,F). Adélie penguins are migratory and usually depart the Palmer area after fledging, while gentoo penguins are nonmigratory and require food in this region beyond March. There are no foraging data post-fledging, but gentoo penguins likely increase foraging dive depths in March to match the depth of the prey field.

Conclusions

Ongoing environmental change along the West Antarctic Peninsula is expected to impact krill recruitment and penguin foraging dynamics in the Palmer Station area. Water column stratification and phytoplankton concentration do not appear to impact the krill biomass present on a given day in the Palmer area; however, bottom-up processes drive krill recruitment success or failure over interannual scales (Saba et al. 2014). Long-term warming, sea ice declines, and increasing wind speeds cause MLDs to deepen and phytoplankton concentrations to decline and shift to smaller cells (Montes-Hugo et al. 2009), which could lead to sustained poor krill recruitment over longer time scales. Decreased krill recruitment could lead to greater seasonal fluctuations in krill abundance near penguin colonies. Warmer waters and less sea ice habitat could also detrimentally impact krill growth and lipid accumulation (Ruck et al. 2014; Klein et al. 2018). Less consistent krill availability and reduced prey quality may result in increased penguin foraging efforts (e.g., longer foraging trip durations, deeper dives). The transition from Adélie to gentoo penguins in the region might shift the demand for krill later in the summer based on differences in breeding phenology and increase the need for seasonally sustained krill to accommodate a nonmigratory local population. However, gentoo penguins have a more diverse diet than Adélie penguins, and alternate prey options could potentially support their needs when local krill availability is low (Pickett et al. 2018).

This study highlights large temporal and spatial variability in krill distributions over the scales relevant to foraging penguins in the Palmer Station vicinity (e.g., differences in krill swarming behavior within regions only 10 km apart). This emphasizes the importance of high-resolution data sets in studying predator foraging ecology. Continued full-ecosystem research incorporating organismal life-history strategies is imperative for understanding the underlying factors that structure coastal biological hotspots and how further environmental change will impact them.

References

- Atkinson, A., and others. 2019. Krill (*Euphausia superba*) distribution contracts southward during rapid regional warming. *Nat. Clim. Chang.* **9**: 142–147. doi:10.1038/s41558-018-0370-z
- Bernard, K. S., and D. K. Steinberg. 2013. Krill biomass and aggregation structure in relation to tidal cycle in a penguin foraging region off the Western Antarctic Peninsula. *ICES J. Mar. Sci.* **70**: 834–849. doi:10.1093/icesjms/fst088
- Bernard, K. S., and others. 2017. Factors that affect the near-shore aggregations of Antarctic krill in a biological hotspot. *Deep. Res. Part I* **126**: 139–147. doi:10.1016/j.dsr.2017.05.008
- Bernard, K. S., and others. 2018. The contribution of ice algae to the winter energy budget of juvenile Antarctic krill in

- years with contrasting sea ice conditions. *ICES J. Mar. Sci.* **76**: 206–216. doi:[10.1093/icesjms/fsy145](https://doi.org/10.1093/icesjms/fsy145)
- Bost, C. A., J. Lage, and K. Putz. 1994. Maximum diving depth and diving patterns of the gentoo penguin *Pygoscelis papua* at the Crozet Islands. *Mar. Ornithol.* **22**: 237–244.
- Carvalho, F., J. Kohut, M. J. Oliver, R. M. Sherrel, and O. Schofield. 2016. Mixing and phytoplankton dynamics in a submarine canyon in the West Antarctic Peninsula. *J. Geophys. Res. Ocean.* **121**: 5069–5083. doi:[10.1002/2016JC011650](https://doi.org/10.1002/2016JC011650)
- Carvalho, F., J. Kohut, M. J. Oliver, and O. Schofield. 2017. Defining the ecologically relevant mixed-layer depth for Antarctica's coastal seas. *Geophys. Res. Lett.* **44**: 338–345. doi:[10.1002/2016GL071205](https://doi.org/10.1002/2016GL071205)
- Carvalho, F., and others. 2019. Testing the Canyon Hypothesis: Evaluating light and nutrient controls of phytoplankton growth in penguin foraging hotspots along the West Antarctic Peninsula. *Limnol. Oceanogr.* **65**: 455–470. doi:[10.1002/lno.11313](https://doi.org/10.1002/lno.11313)
- Chapman, E. W., E. E. Hofmann, D. L. Patterson, and W. R. Fraser. 2010. The effects of variability in Antarctic krill (*Euphausia superba*) spawning behavior and sex/maturity stage distribution on Adélie penguin (*Pygoscelis adeliae*) chick growth: A modeling study. *Deep. Res. Part II* **57**: 543–558. doi:[10.1016/j.dsr2.2009.10.005](https://doi.org/10.1016/j.dsr2.2009.10.005)
- Chapman, E. W., E. E. Hofmann, D. L. Patterson, C. A. Ribic, and W. R. Fraser. 2011. Marine and terrestrial factors affecting Adélie penguin *Pygoscelis adeliae* chick growth and recruitment off the western Antarctic Peninsula. *Mar. Ecol. Prog. Ser.* **436**: 273–289. doi:[10.3354/meps09242](https://doi.org/10.3354/meps09242)
- Cimino, M. A., W. R. Fraser, D. L. Patterson-Fraser, V. S. Saba, and M. J. Oliver. 2014. Large-scale climate and local weather drive interannual variability in Adélie penguin chick fledging mass. *Mar. Ecol. Prog. Ser.* **513**: 253–268. doi:[10.3354/meps10928](https://doi.org/10.3354/meps10928)
- Cimino, M. A., M. A. Moline, W. R. Fraser, D. L. Patterson-Fraser, and M. J. Oliver. 2016. Climate-driven sympatry may not lead to foraging competition between congeneric top-predators. *Sci. Rep.* **6**: 18820. doi:[10.1038/srep18820](https://doi.org/10.1038/srep18820)
- Cleary, A. C., E. G. Durbin, M. C. Casas, and M. Zhou. 2016. Winter distribution and size structure of Antarctic krill *Euphausia superba* populations in-shore along the West Antarctic Peninsula. *Mar. Ecol. Prog. Ser.* **552**: 115–129. doi:[10.3354/meps11772](https://doi.org/10.3354/meps11772)
- Conroy, J. A., C. S. Reiss, M. R. Gleiber, and D. K. Steinberg. 2020. Linking Antarctic krill larval supply and recruitment along the Antarctic Peninsula. *Integr. Comp. Biol.* **60**: 1386–1400. doi:[10.1093/icb/icaa111](https://doi.org/10.1093/icb/icaa111)
- Conti, S. G., and D. A. Demer. 2006. Improved parameterization of the SDWBA for estimating krill target strength. *ICES J. Mar. Sci.* **63**: 928–935. doi:[10.1016/j.icesjms.2006.02.007](https://doi.org/10.1016/j.icesjms.2006.02.007)
- Cook, A. J., P. R. Holland, M. P. Meredith, T. Murray, A. Luckman, and D. G. Vaughan. 2016. Ocean forcing of glacier retreat in the western Antarctic Peninsula. *Science* **353**: 283–286. doi:[10.1126/science.aae0017](https://doi.org/10.1126/science.aae0017)
- Couto, N., D. G. Martinson, J. Kohut, and O. Schofield. 2017. Distribution of upper circumpolar deep water on the warming continental shelf of the West Antarctic Peninsula. *J. Geophys. Res. Ocean.* **122**: 5306–5315. doi:[10.1002/2017JC012840](https://doi.org/10.1002/2017JC012840)
- Daly, K. L., and M. C. Macaulay. 1988. Abundance and distribution of krill in the ice edge zone of the Weddell Sea, austral spring 1983. *Deep Sea Res. Part A Oceanogr. Res. Pap.* **35**: 21–41. doi:[10.1016/0198-0149\(88\)90055-6](https://doi.org/10.1016/0198-0149(88)90055-6)
- Diner, N. 2001. Correction on school geometry and density: Approach based on acoustic image simulation. *Aquat. Living Resour.* **14**: 211–222. doi:[10.1016/S0990-7440\(01\)01121-4](https://doi.org/10.1016/S0990-7440(01)01121-4)
- Emslie, S. D. 2001. Radiocarbon dates from abandoned penguin colonies in the Antarctic Peninsula region. *Antarct. Sci.* **13**: 289–295. doi:[10.1017/S0954102001000414](https://doi.org/10.1017/S0954102001000414)
- Fielding, S., J. L. Watkins, M. A. Collins, P. Enderlein, and H. J. Venables. 2012. Acoustic determination of the distribution of fish and krill across the Scotia Sea in spring 2006, summer 2008 and autumn 2009. *Deep Sea Res. Part II* **59–60**: 173–188. doi:[10.1016/j.dsr2.2011.08.002](https://doi.org/10.1016/j.dsr2.2011.08.002)
- Fielding, S., J. L. Watkins, P. N. Trathan, P. Enderlein, C. M. Waluda, G. Stowasser, G. A. Tarling, and E. J. Murphy. 2014. Interannual variability in Antarctic krill (*Euphausia superba*) density at South Georgia, Southern Ocean: 1997–2013. *ICES J. Mar. Sci.* **71**: 2578–2588. doi:[10.1093/icesjms/fsu104](https://doi.org/10.1093/icesjms/fsu104)
- Folt, C. L., and C. W. Burns. 1999. Biological drivers of zooplankton patchiness. *Trends Ecol. Evol.* **14**: 300–305. doi:[10.1016/S0169-5347\(99\)01616-X](https://doi.org/10.1016/S0169-5347(99)01616-X)
- Foote, K. G. 1990. Spheres for calibrating an eleven-frequency acoustic measurement system. *J. Cons. Int. Explor. Mer.* **46**: 284–286. doi:[10.1093/icesjms/46.3.284](https://doi.org/10.1093/icesjms/46.3.284)
- Fraser, W. R., and W. Z. Trivelpiece. 1996. Factors controlling the distribution of seabirds: Winter-summer heterogeneity in the distribution of Adélie penguin populations, p. 257–272. *In* R. M. Ross, E. E. Hofmann, and L. B. Quetin [eds.], Foundations for ecological research west of the Antarctic Peninsula. Antarctic Research Series: American Geophysical Union. doi:[10.1029/AR070p0257](https://doi.org/10.1029/AR070p0257)
- Fraser, W. R., and E. E. Hofmann. 2003. A predator's perspective on causal links between climate change, physical forcing and ecosystem response. *Mar. Ecol. Prog. Ser.* **265**: 1–15. doi:[10.3354/meps265001](https://doi.org/10.3354/meps265001)
- Fraser, W. R., H. W. Ducklow, and S. F. Henley. 2020. Corrigendum to “Variability and change in the West Antarctic Peninsula marine system: Research priorities and opportunities” [Progr. Oceanogr. (2019) 208–237]. *Prog. Oceanogr.* **186**: 102350. doi:[10.1016/j.pocean.2020.102350](https://doi.org/10.1016/j.pocean.2020.102350)
- Gibbons, M. J., V. A. Spiridonov, and G. A. Tarling. 1999. Euphausiacea, p. 1241–1279. *In* D. Boltovskoy [ed.], South Atlantic zooplankton. Backhuys Publishers.

- Hamner, W. M., and P. P. Hamner. 2000. Behavior of Antarctic krill (*Euphausia superba*): Schooling, foraging, and antipredatory behavior. *Can. J. Fish. Aquat. Sci.* **57**: 192–202.
- Hays, G. C. 2003. A review of the adaptive significance and ecosystem consequences of zooplankton diel vertical migrations, p. 163–170. *In* M. B. Jones, A. Ingólfsson, E. Ólafsson, G. V. Helgason, K. Gunnarsson, and J. Svavarsson [eds.], *Migrations and dispersal of marine organisms. Developments in Hydrobiology* Springer. **174**. doi:10.1007/978-94-017-2276-6_18
- Hewitt, R. P., and others. 2004. Biomass of Antarctic krill in the Scotia Sea in January/February 2000 and its use in revising an estimate of precautionary yield. *Deep. Res. Part II* **51**: 1215–1236. doi:10.1016/j.dsr2.2004.06.011
- Kavanaugh, M. T., and others. 2015. Effect of continental shelf canyons on phytoplankton biomass and community composition along the western Antarctic Peninsula. *Mar. Ecol. Prog. Ser.* **524**: 11–26. doi:10.3354/meps11189
- Klein, E. S., S. L. Hill, J. T. Hinke, T. Phillips, and G. M. Watters. 2018. Impacts of rising sea temperature on krill increase risks for predators in the Scotia Sea. *PLoS One* **13**: e0191011. doi:10.1371/journal.pone.0191011
- Klevjer, T. A., G. A. Tarling, and S. Fielding. 2010. Swarm characteristics of Antarctic krill *Euphausia superba* relative to the proximity of land during summer in the Scotia Sea. *Mar. Ecol. Prog. Ser.* **409**: 157–170. doi:10.3354/meps08602
- Kohut, J. T., P. Winsor, H. Statscewich, M. J. Oliver, E. Fredj, N. Couto, K. Bernard, and W. Fraser. 2018. Variability in summer surface residence time within a West Antarctic Peninsula biological hotspot. *Philos. Trans. R. Soc. A* **376**: 20170165. doi:10.1098/rsta.2017.0165
- Lawson, G. L., P. H. Wiebe, T. K. Stanton, and C. J. Ashjian. 2008. Euphausiid distribution along the Western Antarctic Peninsula—Part A: Development of robust multi-frequency acoustic techniques to identify euphausiid aggregations and quantify euphausiid size, abundance, and biomass. *Deep. Res. Part II Top. Stud. Oceanogr.* **55**: 412–431. doi:10.1016/j.dsr2.2007.11.014
- Lorbacher, K., D. Dommenges, P. P. Niiler, and A. Köhl. 2006. Ocean mixed layer depth: A subsurface proxy of ocean-atmosphere variability. *J. Geophys. Res.* **111**: C07010. doi:10.1029/2003JC002157
- Mauchline, J. 1980. Measurement of body length of *Euphausia superba* Dana, p. 1–9. *In* BIOMASS handbook, no. 4. Scientific Committee Antarctic Research.
- Miller, D. G. M., and I. Hampton. 1989. Krill aggregation characteristics: Spatial distribution patterns from hydroacoustic observations. *Polar Biol.* **10**: 125–134. doi:10.1007/BF00239157
- Miller, A. K., M. A. Kappes, S. G. Trivelpiece, and W. Z. Trivelpiece. 2010. Foraging-niche separation of breeding gentoo and chinstrap penguins, South Shetland Islands, Antarctica. *Condor* **112**: 683–695. doi:10.1525/cond.2010.090221
- Mitchell, G. B., and O. Holm-Hansen. 1991. Bio-optical properties of Antarctic Peninsula waters: Differentiation from temperate ocean models. *Deep Sea Res.* **38**: 1009–1028. doi:10.1016/0198-0149(91)90094-V
- Moline, M. A., and B. B. Prézelin. 1996. Long-term monitoring and analyses of physical factors regulating variability in coastal Antarctic phytoplankton biomass, in situ productivity and taxonomic composition over subseasonal, seasonal and interannual time scales. *Mar. Ecol. Prog. Ser.* **145**: 143–160. doi:10.3354/meps145143
- Montes-Hugo, M., S. C. Doney, H. H. Ducklow, W. Fraser, D. Martinson, S. E. Stammerjohn, and O. Schofield. 2009. Recent changes in phytoplankton communities associated with rapid regional climate change along the Western Antarctic Peninsula. *Science* **323**: 1470–1473. doi:10.1126/science.1164533
- Nicol, S. 2006. Krill, currents, and sea ice: *Euphausia superba* and its changing environment. *Bioscience* **56**: 111–120 doi:10.1641/0006-3568(2006)056[0111:KCASIE]2.0.CO;2.
- Oliver, M. J., A. Irwin, M. A. Moline, W. Fraser, D. Patterson, O. Schofield, and J. Kohut. 2013. Adélie penguin foraging location predicted by tidal regime switching. *PLoS One* **8**: e55163. doi:10.1371/journal.pone.0055163
- Oliver, M. J., and others. 2019. Central place foragers select ocean surface convergent features despite differing foraging strategies. *Sci. Rep.* **9**: 1–10. doi:10.1038/s41598-018-35901-7
- Pickett, E. P., W. R. Fraser, D. L. Patterson-Fraser, M. A. Cimino, L. G. Torres, and A. S. Friedlaender. 2018. Spatial niche partitioning may promote coexistence of *Pygoscelis* penguins as climate-induced sympatry occurs. *Ecol. Evol.* **8**: 9764–9778. doi:10.1002/ece3.4445
- Reiss, C. S., A. M. Cossio, V. Loeb, and D. A. Demer. 2008. Variations in the biomass of Antarctic krill (*Euphausia superba*) around the South Shetland Islands, 1996–2006. *ICES J. Mar. Sci.* **65**: 497–508. doi:10.1093/icesjms/fsn033
- Reiss, C. S., and others. 2017. Overwinter habitat selection by Antarctic krill under varying sea-ice conditions: Implications for top predators and fishery management. *Mar. Ecol. Prog. Ser.* **568**: 1–16. doi:10.3354/meps12099
- Ross, R. M., E. E. Hofmann, and L. B. Quetin [eds.]. 1996a. Foundations for ecological research west of the Antarctic Peninsula. Antarctic Research Series American Geophysical Union. **70**. doi:10.1029/AR070
- Ross, R. M., L. B. Quetin, and C. M. Lascara. 1996b. Distribution of Antarctic krill and dominant zooplankton west of the Antarctic Peninsula, p. 199–217. *In* R. M. Ross, E. E. Hofmann, and L. B. Quetin [eds.], *Foundations for ecological research west of the Antarctic Peninsula*. Antarctic Research Series: American Geophysical Union. **70**. doi:10.1029/AR070p0199
- Ross, R. M., L. B. Quetin, T. Newberger, C. T. Shaw, J. L. Jones, S. A. Oakes, and K. J. Moore. 2014. Trends, cycles, inter-annual variability for three pelagic species west of the

- Antarctic Peninsula 1993–2008. *Mar. Ecol. Prog. Ser.* **515**: 11–32. doi:[10.3354/meps10965](https://doi.org/10.3354/meps10965)
- Ruck, K. E., D. K. Steinberg, and E. A. Canuel. 2014. Regional differences in quality of krill and fish as prey along the Western Antarctic Peninsula. *Mar. Ecol. Prog. Ser.* **509**: 39–55. doi:[10.3354/meps10868](https://doi.org/10.3354/meps10868)
- Saba, G. K., and others. 2014. Winter and spring controls on the summer food web of the coastal West Antarctic Peninsula. *Nat. Commun.* **5**: 4318. doi:[10.1038/ncomms5318](https://doi.org/10.1038/ncomms5318)
- Sailley, S. F., H. W. Ducklow, H. V. Moeller, W. R. Fraser, O. M. Schofield, D. K. Steinberg, L. M. Garzio, and S. C. Doney. 2013. Carbon fluxes and pelagic ecosystem dynamics near two western Antarctic Peninsula Adélie penguin colonies: An inverse model approach. *Mar. Ecol. Prog. Ser.* **492**: 253–272. doi:[10.3354/meps10534](https://doi.org/10.3354/meps10534)
- Santora, J. A., and C. S. Reiss. 2011. Geospatial variability of krill and top predators within an Antarctic submarine canyon system. *Mar. Biol.* **158**: 2527–2540. doi:[10.1007/s00227-011-1753-0](https://doi.org/10.1007/s00227-011-1753-0)
- Schmidt, K., and others. 2011. Seabed foraging by Antarctic krill: Implications for stock assessment, benthic-pelagic coupling, and the vertical transfer of iron. *Limnol. Oceanogr.* **56**: 1411–1428. doi:[10.4319/lo.2011.56.4.1411](https://doi.org/10.4319/lo.2011.56.4.1411)
- Schofield, O., M. Brown, J. Kohut, S. Nardelli, G. Saba, N. Waite, and H. Ducklow. 2018. Changes in the upper ocean mixed layer and phytoplankton productivity along the West Antarctic peninsula. *Philos. Trans. R. Soc. A* **376**: 20170173. doi:[10.1098/rsta.2017.0173](https://doi.org/10.1098/rsta.2017.0173)
- Siegel, V. 1988. A concept of seasonal variation of krill (*Euphausia superba*) distribution and abundance west of the Antarctic Peninsula, p. 219–230. *In* D. Sahrhage [ed.], *Antarctic ocean and resources variability*. Springer. doi:[10.1007/978-3-642-73724-4_19](https://doi.org/10.1007/978-3-642-73724-4_19)
- Siegel, V., C. S. Reiss, K. S. Dietrich, M. Haraldsson, and G. Rohardt. 2013. Distribution and abundance of Antarctic krill (*Euphausia superba*) along the Antarctic Peninsula. *Deep. Res. Part I Oceanogr. Res. Pap.* **77**: 63–74. doi:[10.1016/j.dsr.2013.02.005](https://doi.org/10.1016/j.dsr.2013.02.005)
- Silk, J. R. D., S. E. Thorpe, S. Fielding, E. J. Murphy, P. N. Trathan, J. L. Watkins, and S. L. Hill. 2016. Environmental correlates of Antarctic krill distribution in the Scotia Sea and southern Drake Passage. *ICES J. Mar. Sci.* **73**: 2288–2301. doi:[10.1093/icesjms/fsw097](https://doi.org/10.1093/icesjms/fsw097)
- Stammerjohn, S., R. Massom, D. Rind, and D. Martinson. 2012. Regions of rapid sea ice change: An inter-hemispheric seasonal comparison. *Geophys. Res. Lett.* **39**: L06501. doi:[10.1029/2012GL050874](https://doi.org/10.1029/2012GL050874)
- Steinberg, D. K., and others. 2015. Long-term (1993–2013) changes in macrozooplankton off the Western Antarctic Peninsula. *Deep. Res. Part I* **101**: 54–70. doi:[10.1016/j.dsr.2015.02.009](https://doi.org/10.1016/j.dsr.2015.02.009)
- Taki, K., T. Hayashi, and M. Naganobu. 2005. Characteristics of seasonal variation in diurnal vertical migration and aggregation of Antarctic krill (*Euphausia superba*) in the Scotia Sea, using Japanese fishery data. *CCAMLR Sci.* **12**: 163–172.
- Tarling, G. A., and others. 2009. Variability and predictability of Antarctic krill swarm structure. *Deep. Res. Part I* **56**: 1994–2012. doi:[10.1016/j.dsr.2009.07.004](https://doi.org/10.1016/j.dsr.2009.07.004)
- Tarling, G. A., S. E. Thorpe, S. Fielding, T. Klevjer, A. Ryabov, and P. J. Somerfield. 2018. Varying depth and swarm dimensions of open-ocean Antarctic krill *Euphausia superba* Dana, 1850 (Euphausiacea) over diel cycles. *J. Crustac. Biol.* **38**: 716–727. doi:[10.1093/jcbiol/ruy040](https://doi.org/10.1093/jcbiol/ruy040)
- Trivelpiece, W. Z., S. G. Trivelpiece, and N. J. Volkman. 1987. Ecological segregation of Adélie, gentoo, and chinstrap penguins at King George Island, Antarctica. *Ecology* **68**: 351–361. doi:[10.2307/1939266](https://doi.org/10.2307/1939266)
- Vernet, M., D. Martinson, R. Iannuzzi, S. Stammerjohn, W. Kozłowski, K. Sines, R. Smith, and I. Garibotti. 2008. Primary production within the sea-ice zone west of the Antarctic Peninsula: I—Sea ice, summer mixed layer, and irradiance. *Deep. Res. Part II* **55**: 2068–2085. doi:[10.1016/j.dsr2.2008.05.021](https://doi.org/10.1016/j.dsr2.2008.05.021)
- Volkman, N. J., P. Presler, and W. Trivelpiece. 1980. Diets of Pygoscelid penguins at King George Island, Antarctica. *Condor* **82**: 373–378. doi:[10.2307/1367558](https://doi.org/10.2307/1367558)
- Walsh, J., C. S. Reiss, and G. M. Watters. 2020. Flexibility in Antarctic krill *Euphausia superba* decouples diet and recruitment from overwinter sea-ice conditions in the northern Antarctic Peninsula. *Mar. Ecol. Prog. Ser.* **642**: 1–19. doi:[10.3354/meps13325](https://doi.org/10.3354/meps13325)
- Watanuki, Y., A. Kato, Y. Naito, G. Robertson, and S. Robinson. 1997. Diving and foraging behaviour of Adélie penguins in areas with and without fast sea-ice. *Polar Biol.* **17**: 296–304. doi:[10.1007/PL00013371](https://doi.org/10.1007/PL00013371)
- Wiebe, P. H., D. Chu, S. Kaartvedt, A. Hundt, W. Melle, E. Ona, and P. Batta-Lona. 2010. The acoustic properties of *Salpa thompsoni*. *ICES J. Mar. Sci.* **67**: 583–593. doi:[10.1093/icesjms/fsp263](https://doi.org/10.1093/icesjms/fsp263)
- Williams, T. D. 1995. *The penguins*. . . Oxford University Press.
- Xing, X., H. Claustre, S. Blain, F. D’Ortenzio, D. Antoine, J. Ras, and C. Guinet. 2012. Quenching correction for in vivo chlorophyll fluorescence acquired by autonomous platforms: A case study with instrumented elephant seals in the Kerguelen region (Southern Ocean). *Limnol. Oceanogr. Methods* **10**: 483–495. doi:[10.4319/lom.2012.10.483](https://doi.org/10.4319/lom.2012.10.483)

Acknowledgments

This work was supported by the National Science Foundation Antarctic Organisms and Ecosystems Program (PLR-1440435) as part of the Palmer Antarctica Long-Term Ecological Research (Palmer LTER) program. Additionally, S.N. acknowledges support from the Rutgers Institute of Earth, Ocean, and Atmospheric Sciences graduate fellowship, W.F. acknowledges support from the Detroit Zoological Society and NSF Office of Polar Programs (ANT-1745018), and M.C. acknowledges support from the NSF Office of Polar Programs (ANT-1744859). The Virginia Institute of Marine Science, William & Mary contribution number is 4002. Thank you to

Anthony Cossio and Chris Taylor for sharing acoustic processing code and advice. This work would not be possible without the Palmer LTER field teams who aided in data collection and Palmer Station personnel for logistics support. Comments from two anonymous reviewers helped improve and clarify this manuscript.

Submitted 04 August 2020

Revised 16 January 2021

Accepted 11 March 2021

Associate editor: Thomas Kiørboe

Conflict of Interest

None declared